International Journal of Trend in Research and Development, Volume 13(3), ISSN: 2394-9333
www.ijtrd.com

Interfacial Diffusion in Heat-Treated C276/Q370R Explosion-Welded Clad Plates: A Molecular Dynamics Study

[1]Zhiming Huang, [2]Yuhang Liu and [3]Xuyang Zhao,
[1,2,3]School of Materials Science and Engineering, Henan Polytechnic University, Jiaozuo, China
*Corresponding author

Abstract: To clarify the interfacial diffusion law and mechanism of a C276/Q370R explosion-welded clad plate during post-weld heat treatment, a molecular dynamics model was established and used to analyze atomic migration behavior at the interface. A simplified Fe/Cr/C interfacial system was adopted to capture the dominant thermally activated diffusion trends, and the effects of temperature on atomic distribution, mean square displacement (MSD), concentration profile, interdiffusion width, apparent diffusion coefficient, and activation energy were evaluated. The results show that Fe, Cr, and C atoms remain in a thermally activated diffusion state throughout the simulation, and their migration capability increases monotonically with temperature. As the temperature increases from 700 to 1200 °C, the terminal MSD values of Fe, Cr, and C rise from 1613.42 to 2615.60 $Å^2$, from 1562.08 to 2498.75 $Å^2$, and from 2556.53 to 4062.64 $Å^2$, respectively. The corresponding apparent diffusion coefficients increase from 17.21 to 28.70, from 16.60 to 27.19, and from 27.54 to 44.69 $\times 10^{-7} m^2 s^{-1}$, respectively. The interdiffusion layer width expands from 73.191 to 84.120 Å, while the fraction of carbon redistributed to the Cr-side representative region increases from 14.358% to 18.807%. Arrhenius fitting indicates activation energies of 11.805 $kJ \cdot mol^{-1}$ for Fe, 11.804 $kJ \cdot mol^{-1}$ for Cr, and 11.402 $kJ \cdot mol^{-1}$ for C, confirming that carbon diffusion dominates the interfacial transport process. These results provide an atomistic basis for understanding carbide precipitation, decarburization-layer formation, and interfacial property evolution during heat treatment.

Keywords: *Explosion-welded clad plate; Molecular dynamics; Interfacial diffusion; Heat treatment; C276/Q370R; Carbon migration*

I. INTRODUCTION

Explosion-welded clad plates combine the corrosion resistance of a cladding alloy with the strength and economy of a steel substrate, and they are therefore widely used in corrosive chemical equipment, pressure-bearing structures, and high-temperature service environments. For C276/Q370R clad systems, post-weld heat treatment inevitably induces interfacial atomic interdiffusion, carbon migration across the interface, and subsequent carbide-related microstructural evolution. These processes directly affect interfacial bonding, hardness gradients, and corrosion stability [1-2].

Experimental studies can reveal interfacial evolution through microstructure, elemental distribution, and property variation, but the atomic migration pathways, kinetic hierarchy among different elements, and the thermally activated nature of diffusion remain difficult to resolve directly from experiments alone. Molecular dynamics (MD) is therefore a useful complementary tool, because it can track the spatiotemporal evolution of interfacial atoms at the atomic scale and provide direct kinetic evidence for heat-treatment diffusion and interfacial compositional reconstruction [1-2], [10].

On this basis, the present work addresses the interfacial diffusion behavior of a C276/Q370R explosion-welded clad plate during heat treatment by constructing a simplified Fe/Cr/C MD model. The evolution of atomic distribution, MSD, concentration profiles, interdiffusion width, apparent diffusion coefficients, and Arrhenius parameters is analyzed systematically in order to clarify the dominant diffusion mechanism and to provide theoretical support for subsequent interpretation of carbide precipitation, decarburization-layer formation, and property changes near the interface [1-2], [7-10].

II. MATERIALS AND METHODS

A. Modeling Strategy

The real C276/Q370R interface has a complex multicomponent composition and contains many atomic species. To highlight the dominant law of interfacial diffusion during heat treatment, a strategy of simplified representative elements plus key interstitial carbon was adopted. In the primary model, the C276 side was simplified to Cr as the representative alloy-side element, while the Q370R side was simplified to Fe as the representative steel-side matrix element. In the extended model, a small amount of carbon was introduced near the Fe side of the interface to characterize the coupling between interstitial C migration and substitutional-atom diffusion. This strategy is more suitable for identifying relative diffusion trends and dominant mechanisms; the precise cooperative effects of Ni, Mo, and other alloying elements in the real multicomponent system remain beyond the scope of the present simplified simulation and should be treated in a future multicomponent model [1], [3], [4].

B. Model Construction and Simulation Procedure

The interfacial model used a planar interface with the interface normal along the (z)-direction. The Cr side was constructed with an fcc lattice, and the Fe side was constructed with a bcc lattice. To avoid unrealistically large repulsive forces caused by direct contact in the initial configuration, an initial gap of approximately 2 Å was reserved between the two sides of the interface. The model dimensions were 70 Å × 70 Å × 70 Å for the Cr side and 70 Å × 70 Å × 90 Å for the Fe side. Periodic boundary conditions were applied in the (x)- and (y)-directions, while a double-interface configuration was introduced along the (z)-direction to reduce free-surface effects.

The simulation procedure consisted of four stages: energy minimization, structural relaxation, heating/stabilization, and isothermal holding for diffusion sampling. After energy minimization, the system was relaxed in an NPT ensemble at (P = 0) for 20–50 ps, then heated to the target temperature at 5–10

$K \cdot ps^{-1}$, stabilized for 20–50 ps, and finally sampled under isothermal holding for 1–3 ns depending on temperature and diffusion rate. Temperature and pressure control were implemented using the Nosé–Hoover method, and time integration followed the standard MD practice associated with the Verlet/velocity-Verlet family of algorithms [3-6]. No external mechanical load was applied, because the focus of this work is thermally driven diffusion rather than diffusion under coupled thermomechanical loading. The exact integration time step is unspecified in the source text [typically about 1 fs for metallic systems].

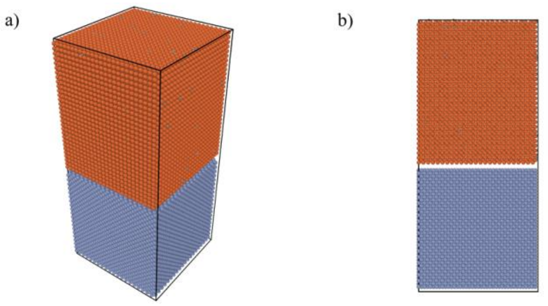

Fig 1Initial Fe–Cr–C interfacial model: (a) three-dimensional view; (b) xoz-plane view.

III. RESULTS AND DISCUSSION

A. Time-Dependent Interdiffusion Behavior

At a fixed temperature, interfacial diffusion exhibits an evident two-stage feature: rapid initial mixing followed by quasi-steady diffusion. In the early stage, atomic migration is enhanced by the high-energy interfacial structure and defect states; in the middle and later stages, the system gradually evolves toward a more stable thermally activated diffusion state.

To quantify this behavior, MSD curves of Fe, Cr, and C atoms were extracted over the temperature range of 700–1200 °C. The MSD can be written as

$$\mathrm{MSD}(t) = \frac{1}{N}\sum_{i=1}^{N} \left|\boldsymbol{r_i}(t) - \boldsymbol{r_i}(0)\right|^2 \#(1)$$

where(N) is the number of atoms considered, and $(r_i(t))$ and $(r_i(0))$ are the position vectors of the(i)-th atom at time (t) and at the initial state, respectively.

The MSD values of Fe, Cr, and C increase continuously with time at all temperatures, which indicates persistent thermally activated interfacial diffusion. The initial part of each curve shows a relatively nonlinear feature, mainly associated with heating and the establishment of thermal equilibrium; with longer simulation time, the curves become more linear, indicating that the interface enters a more stable diffusion regime. A comparison among atomic species shows that the MSD of C is always significantly higher than those of Fe and Cr, while Fe is slightly more mobile than Cr. This hierarchy indicates that interstitial carbon is the most active diffusing species, whereas Fe and Cr, as substitutional atoms, diffuse more slowly. This trend is consistent with broader MD observations for Fe self-diffusion and carbon transport in iron-based systems.

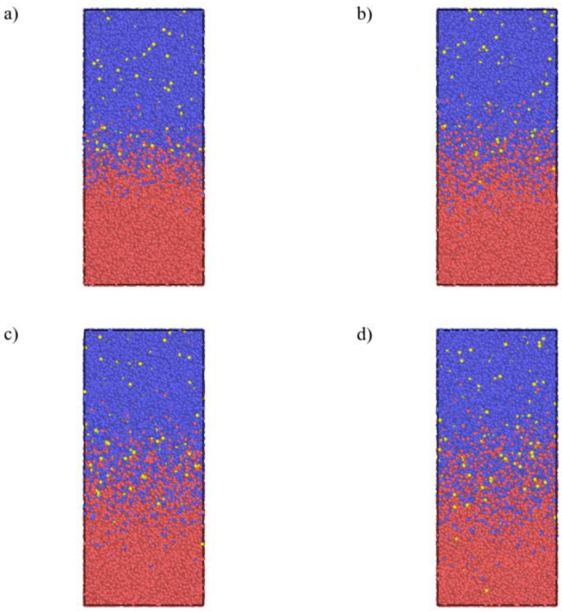

Fig 2Atomic distribution at the Fe/Cr interface at 900 °C under different simulation steps: (a) 5000 steps; (b) 10000 steps; (c) 15000 steps; (d) 20000 steps.

Table 1: Terminal MSD of each element at the end of simulation

Temperature / °C	Fe terminal MSD / Å(^2)/ Å²	Cr terminal MSD / Å²	C terminal MSD / Å²
700	1613.42	1562.08	2556.53
800	1825.27	1747.38	2879.51
900	1990.16	1932.73	3154.86
1000	2177.33	2141.43	3455.88
1100	2361.91	2306.91	3748.78
1200	2615.60	2498.75	4062.64

From the diffusion-time perspective, the interfacial diffusion process therefore presents clear stage dependence: the early stage is strongly affected by heating and structural adjustment, while the later stage increasingly reflects stable thermally activated diffusion. At the same time, the diffusion rates of different atomic species remain substantially different, with carbon showing the highest mobility, Fe the second highest, and Cr the lowest.

B. Temperature-Dependent Concentration Redistribution

To further analyze the effect of temperature on interfacial diffusion, the final concentration distributions after simulation were statistically evaluated at 700, 800, 900, 1000, 1100, and 1200 °C, and then interpreted together with the MSD results.

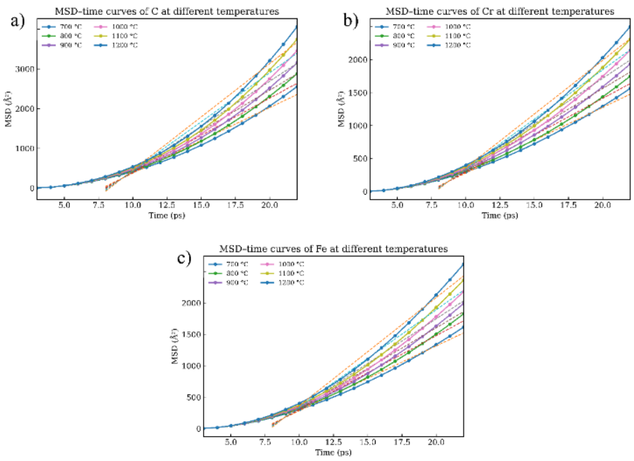

Fig 3 MSD–time curves of different atoms at different temperatures: (a) C; (b) Cr; (c) Fe.

Near the interface, Fe and Cr both form a distinct compositional transition zone. Using the concentration ratio to characterize Fe–Cr inter diffusion shows that the interfacial transition layer broadens gradually as temperature increases. At the same time, the interface center remains approximately stable within the range of 76–78 Å, indicating that the major temperature effect is the widening of the concentration-gradient region rather than an overall shift of interface position. This type of heat-treatment-induced layer broadening is also consistent with interfacial diffusion observations reported for related Hastelloy/steel bimetal systems.

Carbon exhibits stronger temperature sensitivity than the substitutional elements. The statistics show that C atoms are mainly enriched on the Fe-rich side overall, but their fraction transported to the Cr-side representative region increases continuously with temperature. This indicates progressively more sufficient cross-interface carbon transport at elevated temperature.

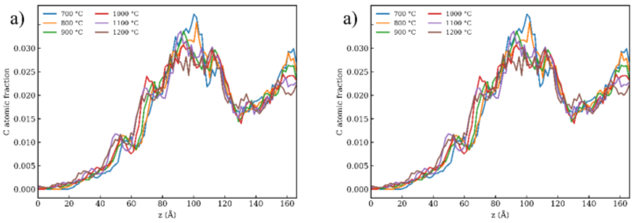

Fig 4Element concentration distributions at different temperatures: (a) C; (b) Cr/(Cr + Fe).

Combined with the existing microstructural observations of the project, this result supports the view that carbide precipitation near the interface is mainly promoted on the alloy side adjacent to the interface.

Table 2 Interfacial concentration-profile parameters at different temperatures

Temperature / ℃	Interface center $x_{0.5}$ / Å	Interdiffusion width / Å	C on Cr side / %	C on Fe side/ %
700	77.960	73.191	14.358	85.642
800	77.384	73.550	16.279	83.721
900	76.301	76.296	15.571	84.429
1000	77.569	79.160	17.391	82.609
1100	78.407	82.189	19.211	80.789
1200	78.142	84.120	18.807	81.193

As temperature rises, carbon migration from the steel side toward the alloy side becomes more pronounced, thereby providing more favorable conditions for the combination of C with strong carbide-forming elements such as Cr and Mo in the actual alloy system. Thus, from the temperature perspective, heating not only strengthens Fe, Cr, and C diffusion in general, but also strongly enhances transition-layer widening and carbon redistribution across the interface; carbon remains the key controlling factor in interfacial compositional reconstruction and subsequent carbide precipitation.

C. Apparent Diffusion Coefficients and Activation Energies

According to the Einstein diffusion relation, the apparent diffusion coefficient under three-dimensional conditions can be obtained from the slope of the MSD curve:

$$D = \frac{1}{6}\frac{d(\mathrm{MSD})}{dt} \#(2)$$

Considering the influence of heating and structural relaxation in the early part of the simulation, the linear fitting was performed over the 8–22 ps interval so as to reduce the effect of the non-steady stage. It should be emphasized that, because the present script accumulates MSD during heating, the resulting (D) values are better interpreted as apparent diffusion capabilities under different terminal temperatures rather than strict steady-state tracer diffusivities.

Table 3Apparent diffusion coefficients of interfacial atoms at different temperatures

Temperature / ℃	$\boldsymbol{D}_{\mathrm{Fe}}$ / (× 10−7m2s−1)	$\boldsymbol{D}_{\mathrm{C}\boldsymbol{r}}$ / (× 10−7m2s−1)	$\boldsymbol{D}_{\mathrm{C}}$ / (× 10−7m2s−1)
700	1.7208	1.6601	2.7537
800	1.9643	1.8647	3.1235
900	2.1516	2.0842	3.4361
1000	2.3676	2.3119	3.7787
1100	2.5792	2.5052	4.1116
1200	2.8699	2.7189	4.4687

All three diffusion coefficients increase monotonically from 700 to 1200 °C, confirming that temperature is the dominant variable controlling interfacial diffusion. The diffusion coefficient of carbon is always substantially higher than those of Fe and Cr, in full agreement with the MSD analysis. This result is physically reasonable, because interstitial carbon migration in iron-based lattices is known to be markedly faster than substitutional diffusion, while Fe self-diffusion and Cr-like substitutional motion require higher cooperative atomic rearrangement.

To further evaluate the thermally activated character of interfacial diffusion, the calculated diffusion coefficients were fitted using the Arrhenius relation:

$$D = D_0 \exp\left(-\frac{Q}{RT}\right) \#(3)$$

or, after taking logarithms,

$$\ln D = \ln D_0 - \frac{Q}{RT} \#(4)$$

where (D_0) is the pre-exponential factor, (Q) is the activation energy, (R) is the gas constant, and (T) is the thermodynamic temperature.

The fitted activation energies of Fe and Cr are nearly identical, whereas carbon shows the lowest activation energy and the largest pre-exponential factor. This confirms that carbon diffusion is the most sensitive and kinetically favored process at the interface.

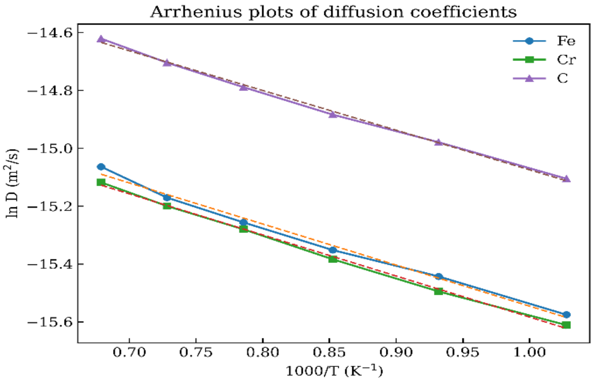

Fig 5Arrhenius fits of interfacial atomic diffusion coefficients.

In other words, interfacial transport in the present system is controlled less by a strong divergence between Fe and Cr mobility and more by the dominant role of interstitial carbon redistribution.

Table 4 Arrhenius fitting parameters of interfacial atomic diffusion

Diffusing species	Q / kJ·mol^-1	Q / eV·atom^-1	D_0 / m^2·s^-1
Fe	11.805	0.1223	7.3312×10^-7
Cr	11.804	0.1223	7.0589×10^-7
C	11.402	0.1182	1.1188×10^-6

For later-stage real-material evolution, this is especially important because carbon migration provides the kinetic basis for carbide formation and chemical heterogeneity across the true C276/Q370R interface.

CONCLUSION

A simplified Fe/Cr/C molecular dynamics model was established to study interfacial diffusion in a C276/Q370R explosion-welded clad plate during heat treatment. Within the temperature range of 700–1200 °C, Fe, Cr, and C all remain in a thermally activated diffusion state, and their mobility increases monotonically with temperature.

The diffusion process exhibits an obvious staged character. In the initial stage, diffusion is strongly influenced by heating and structural adjustment; with increasing time, the system gradually enters a more stable diffusion regime. Among the three atomic species, carbon always shows the highest MSD and the largest apparent diffusion coefficient, followed by Fe and then Cr.

Temperature increase leads to significant broadening of the Fe–Cr interdiffusion zone, with the interfacial width increasing from 73.191 to 84.120 Å. At the same time, carbon redistribution across the interface becomes more obvious, and the carbon fraction on the Cr-side representative region increases from 14.358% to 18.807%.

Arrhenius analysis shows that the activation energies of Fe, Cr, and C are 11.805, 11.804, and 11.402 $kJ \cdot mol^{-1}$, respectively. The lower activation energy and higher mobility of carbon confirm that cross-interface carbon transport is the dominant kinetic factor in interfacial compositional reconstruction and provides the atomistic basis for subsequent carbide precipitation, decarburization-layer formation, and related property evolution.

References

[1] Wang X, Wang Y, Li G, et al. Review of molecular dynamics simulation of bimetallic interfacial behavior[J]. Materials, 2025, 18(13): 3048.
[2] Hedayati O, Korei N, Adeli M, et al. Microstructural evolution and interfacial diffusion during heat treatment of Hastelloy/stainless steel bimetals[J]. Journal of Alloys and Compounds, 2017, 712: 172-178.
[3] Daw M S, Baskes M I. Embedded-atom method: Derivation and application to impurities, surfaces, and other defects in metals[J]. Physical Review B, 1984, 29(12): 6443-6453.
[4] Baskes M I. Modified embedded-atom potentials for cubic materials and impurities[J]. Physical Review B, 1992, 46(5): 2727-2742.
[5] Hoover W G. Canonical dynamics: Equilibrium phase-space distributions[J]. Physical Review A, 1985, 31(3): 1695-1697.
[6] Swope W C, Andersen H C, Berens P H, et al. A computer simulation method for the calculation of equilibrium constants for the formation of physical clusters of molecules: Application to small water clusters[J]. The Journal of Chemical Physics, 1982, 76(1): 637-649.
[7] Mendelev M I, Mishin Y. Molecular dynamics study of self-diffusion in bcc Fe[J]. Physical Review B, 2009, 80(14): 144111.
[8] Ishii A, Ogata S, Kimizuka H, et al. Adaptive-boost molecular dynamics simulation of carbon diffusion in iron[J]. Physical Review B, 2012, 85(6): 064303.
[9] Timmerscheidt T A, von Appen J, Dronskowski R. A molecular-dynamics study on carbon diffusion in face-centered cubic iron[J]. Computational Materials Science, 2014, 91: 235-239.
[10] Gu C, Zeng S, Peng W, et al. Molecular dynamic simulation and experiment validation on the diffusion behavior of diffusion welded Fe-Ti by hot isostatic pressing process[J]. Materials, 2023, 16(16): 5626.